© 2017. Published by The Company of Biologists Ltd | Development (2017) 144, 916-927 doi:10.1242/dev.144949

RESEARCH ARTICLE

A novel floor plate boundary defined by adjacent En1 and Dbx1 microdomains distinguishes midbrain dopamine and hypothalamic neurons

Navid Nouri and Rajeshwar Awatramani*

ABSTRACT

The mesodiencephalic floor plate (mdFP) is the source of diverse neuron types. Yet, how this structure is compartmentalized has not been clearly elucidated. Here, we identify a novel boundary subdividing the mdFP into two microdomains, defined by engrailed 1 (*En1*) and developing brain homeobox 1 (*Dbx1*). Utilizing simultaneous dual and intersectional fate mapping, we demonstrate that this boundary is precisely formed with minimal overlap between *En1* and *Dbx1* microdomains, unlike many other boundaries. We show that the *En1* microdomain gives rise to dopaminergic (DA) neurons, whereas the *Dbx1* microdomain gives rise to subthalamic (STN), premammillary (PM) and posterior hypothalamic (PH) populations. To determine whether En1 is sufficient to induce DA neuron production beyond its normal limit, we generated a mouse strain that expresses En1 in the *Dbx1* microdomain. In mutants, we observed ectopic production of DA neurons derived from the *Dbx1* microdomain, at the expense of STN and PM populations. Our findings provide new insights into subdivisions in the mdFP, and will impact current strategies for the conversion of stem cells into DA neurons.

KEY WORDS: Floor plate, Dopamine, Subthalamic, Fate map, Boundary, Mouse, Premammillary

INTRODUCTION

Borders are defined when territorial disputes are resolved. This is also the case in early embryonic CNS development, when neighboring progenitor zones are vying for territory, ultimately settling the conflict by agreement on a boundary (Briscoe and Small, 2015; Dasen and Jessell, 2009; Kiecker and Lumsden, 2005; Prochiantz and Di Nardo, 2015). Typically, diffusible morphogens drive the expression of transcription factors initially in a 'fuzzy' manner, which then through cross-repressive interactions establish sharply defined, molecularly distinct progenitor zones. Accurate settling of these disputes is crucial, as they ultimately determine the numbers and types of neurons produced, with consequent outcomes on physiology and behavior. Recent papers have relied on gene expression patterns and fate mapping, to develop more sophisticated maps of the developing CNS (Bedont et al., 2015; Puelles et al., 2013; Puelles and Rubenstein, 2015; Shimogori et al., 2010; Swanson, 2012; Thompson et al., 2014). Despite significant progress, these recent reviews acknowledge that current models are imperfect and that further evaluation using modern molecular tools is imperative.

Recently, much work has focused on the progenitor zone that gives rise to dopamine (DA) neurons in the midbrain, with a goal of deriving DA neurons from stem cells, for modeling and ultimately treating Parkinson's disease (Arenas et al., 2015; Blaess and Ang, 2015; Smidt and Burbach, 2007; Smits et al., 2006; Studer, 2012). In the developing CNS, DA neurons arise from the mesodiencephalic floor plate (mdFP), here defined by the co-expression of Shh, Foxa2 and Lmx1a rostral to the midbrain-hindbrain boundary (MHB), due to the concerted action of Shh, Fgf and Wnt signaling pathways (Arenas et al., 2015; Blaess and Ang, 2015; Joksimovic and Awatramani, 2014; Lahti et al., 2012; Luo and Huang, 2016; Smits et al., 2006; Wurst and Prakash, 2014). In terms of boundaries delimiting the DA progenitor zone, several studies have demonstrated that the caudal limit of DA neuron production is at the MHB defined by the caudal limit of Otx2 expression (Brodski et al., 2003; Joyner et al., 2000; Simeone et al., 2002). Forced ectopic expression of Otx2 in the hindbrain floor plate (FP) results in DA neuron production in the hindbrain (Ono et al., 2007), whereas loss of Otx1/2 results in expanded hindbrain at the expense of midbrain (Omodei et al., 2008; Puelles et al., 2004; Simeone et al., 2002). Along the dorsoventral (D-V) axis, several studies have demonstrated that the $Shh^{+}/Foxa2^{+}$ domain is subdivided into at least two main domains defined by Lmx1a/b and Nkx6-1/Sim1/Neurog1 (Andersson et al., 2006; Blaess et al., 2011; Hayes et al., 2011; Joksimovic et al., 2009; Nakatani et al., 2010; Nouri et al., 2015; Prakash et al., 2009). The Lmx1a/b domain is the origin of most DA neurons, whereas the Nkx6-1/Sim1/Neurog1 domain is the source of $Pou4f1^{+}$ red nucleus (RN) neurons and other smaller populations. Knockouts of Lmx1a/b results in fewer DA neurons and ectopic $Pou4f1^{+}$ neurons from the DA domain (Deng et al., 2011; Yan et al., 2011), whereas forced ectopic expression of Lmx1a/b result in DA neuron production from the Nkx6-1/Sim1/Neurog1 domain at the expense of RN neurons (Anderegg et al., 2013; Andersson et al., 2006; Lin et al., 2009; Nakatani et al., 2010). Conversely, forced ectopic expression of Sim1 results in the production of $Pou4f1^{+}$ neurons from the Lmx1a/b domain, at the expense of DA neurons (Nakatani et al., 2010). Thus, many studies have characterized the caudal and dorsal boundaries of the DA progenitor zone. In contrast, rostrally, it is not even clear whether there is a boundary in the strict sense, i.e. a lineage-restricted compartment (Kiecker and Lumsden, 2005), or whether DA neuron production merely tapers off, due to lack of fibroblast growth factors or other diffusible signals.

Is the mdFP subdivided into compartments along the anteroposterior (A-P) axis? In the early embryo, differentiating Th^{+} DA neurons are observed in the midbrain with a caudal limit at the MHB. The anterior limit of this Th^{+} DA cohort is approximately near the base of the zona limitans intrathalamica (ZLI), the boundary between presumptive developmental segmental units, prosomeres 2

Department of Neurology, Feinberg School of Medicine, Northwestern University, Chicago, IL 60611, USA.

*Author for correspondence (r-awatramani@northwestern.edu)

R.A., 0000-0002-0713-2140

Received 22 September 2016; Accepted 18 January 2017

Development (2017) 144, 916-927 doi:10.1242/dev.144949

and 3 (p2 and p3) (Joksimovic et al., 2009; Nouri et al., 2015; Puelles and Rubenstein, 2015). Because these neurons appear to be generated from the midbrain as well as presumptive p1, p2 and p3, some have called these mesodiencephalic DA neurons (Puelles and Rubenstein, 2015; Veenvliet and Smidt, 2014), as opposed to midbrain DA neurons (Arenas et al., 2015; Blaess and Ang, 2015). Interestingly, most of the currently known DA progenitor markers, including *Shh*, *Wnt1*, *Otx2*, *Neurog2*, *Lmx1a/b*, *Foxa1/2* and *Msx1*, among others, are expressed rostrally, well beyond the ZLI, into presumptive p3 of the diencephalon (Alvarez-Bolado et al., 2012; Andersson et al., 2006; Ellisor et al., 2012; Lahti et al., 2012; Nouri et al., 2015; Puelles and Rubenstein, 2015). Why DA neurons are not produced from the entire A-P axis of the $Shh^+/Foxa2^+/Lmx1a^+$ mdFP, despite the presence of key signaling molecules and transcription factors, is a conundrum. One possibility is that the mdFP is subdivided along the A-P axis into lineage-restricted microdomains. Such a possibility is indeed depicted in prosomere-based models of the segmentally divided embryonic CNS (Björklund and Dunnett, 2007; Puelles and Rubenstein, 2015; Rubenstein et al., 1994; Smidt and Burbach, 2007; Smits et al., 2006, 2013), but evidence for such microdomains within the $Shh^+/Foxa2^+/Lmx1a^+$ mdFP is limited. These models of the subdivided mdFP are based on prosomeric gene expression patterns in more dorsal CNS structures, and these genes are often not expressed in the mdFP. Thus, it remains open whether the mdFP is a compartmentalized structure. In this regard, studies in more caudal regions of the CNS, such as the hindbrain, demonstrate that the FP does not have segmental divisions both in terms of gene expression and cell mixing capability (Fraser et al., 1990; Seitanidou et al., 1997; Wilkinson et al., 1989). In contrast, the neighboring hindbrain neuroepithelium is the archetype of the segmentally subdivided CNS (Kiecker and Lumsden, 2005).

To test whether the $Shh^+/Foxa2^+/Lmx1a^+$ mdFP is subdivided into microdomains, we examined transcription factors that could potentially segregate this region along the A-P axis. Engrailed 1 (En1) is known to be expressed in the midbrain beginning at about embryonic day (E) 8.0 (Chi et al., 2003; Davis and Joyner, 1988) and encompasses the majority of the DA primordium, excluding a small number of Th^+ neurons at the rostral-most extent (Lahti et al., 2012). Engrailed 1 and 2 (En1/2) are important for DA neuron generation and survival (Alberi et al., 2004; Alvarez-Fischer et al., 2011; Alves dos Santos and Smidt, 2011; Ellisor et al., 2012; Nordström et al., 2015; Rekaik et al., 2015; Simon et al., 2001; Veenvliet et al., 2013). Moreover, engrailed proteins are involved in various boundary formation systems such as the diencephalic-dorsal midbrain boundary (Matsunaga et al., 2000; Scholpp et al., 2003) and a D-V boundary in the limb apical ectodermal ridge (Kimmel et al., 2000). In contrast, developing brain homeobox 1 (Dbx1) expression is excluded from the ventral midbrain, but is expressed in the caudal ventral diencephalon at this stage (Causeret et al., 2011; Shoji et al., 1996; Sokolowski et al., 2016). In the spinal cord, Dbx1 has been shown to repress En1 indirectly (Karaz et al., 2016; Pierani et al., 2001). Taking these previous studies into consideration, we sought to examine these two transcription factors in more detail. We reveal two precisely established and abutting microdomains within the mdFP, their diverse neuronal descendants, and a sufficient role for En1 in expanding DA neuron production along the A-P axis.

RESULTS

The mdFP gives rise to DA and non-DA neuron populations

To define the A-P extent of the mdFP and its derivatives, we examined Foxa2 expression in sagittal sections of *Shh::Cre, RC::NZG* embryos, in which nuclear βgal is activated in the Shh domain (in figures this reporter is referred to as *R.NZG*). Consistent with the literature and our previous observations (Alvarez-Bolado et al., 2012; Echelard et al., 1993; Nouri et al., 2015; Puelles and Rubenstein, 2015), $\beta gal^+/Foxa2^+$ cells are observed in the midbrain, and well rostral to the ZLI, in the diencephalon (Fig. 1A-B′). Rostral to the $\beta gal^+/Foxa2^+$ region, $\beta gal^+/Foxa2^-$ cells are observed. The Shh domain therefore encompasses the Foxa2 domain, but also extends significantly more anteriorly than the Foxa2 domain.

At midbrain levels, Shh/Foxa2 derivatives have been previously described, and include DA and RN populations (Blaess et al., 2011; Hayes et al., 2011; Joksimovic et al., 2009). To identify mdFP derivatives rostral to the midbrain, we examined coronal sections through the rostral midbrain/caudal diencephalon. Foxa2-labeled cells are observed in two streams apparently migrating tangentially from the ventricular zone – one mediolaterally and the other rostrally (Fig. 1C). These $Foxa2^+$ cells are located rostral to Th^+ DA neuron populations. Shh fate maps combined with Foxa2 immunolabeling reveal $YFP^+/Foxa2^+$ cells in the subthalamic (STN), supramammillary (SuM), posterior hypothalamic (PH) and premammillary (PM) nuclei, suggesting that these neuronal populations are derived from the mdFP (Fig. 1D-K″).

We next examined the A-P extent of Foxa2 and Lmx1a expression in relation to DA neuron production from the mdFP (Fig. 2A-C‴). In mid-sagittal sections of E9.5-E12.5 embryos, Foxa2 and Lmx1a are co-expressed at the midline; Th^+ DA neurons are observed in the midbrain, but are excluded from more rostral portions of the $Foxa2^+/Lmx1a^+$ domain. This observation led us to hypothesize that the mdFP is subdivided along the A-P axis into two microdomains – one giving rise to DA neurons, and a second giving rise to non-DA neurons. To investigate this hypothesis, we searched for genes in the literature, particularly transcription factors expressed early in development that could subdivide the mdFP in a meaningful manner towards early CNS patterning. Consistent with previous reports (Davis and Joyner, 1988; Simon et al., 2001), we found the transcription factor *En1* expressed in the early ventral midbrain (Fig. 2D). In contrast, the transcription factor *Dbx1* was expressed in the ventral diencephalon, but appeared to be excluded from the ventral midbrain (Fig. 2D′) (Causeret et al., 2011; Shoji et al., 1996). These factors appear to subdivide the mdFP along the A-P axis at E9, although at later stages a gap between these two domains is observed, probably owing to the dynamic expression of these factors (Fig. S1).

To correlate these two progenitor domains with possible postmitotic neuron markers, we examined the expression of two markers, *Pitx3* and *Pitx2* (Martin et al., 2004; Smidt et al., 1997). Our analysis revealed adjacent, non-overlapping populations of $Pitx3^+$ DA and $Pitx2^+$ non-DA neurons (Fig. 2E,E′). We also observed $Pitx2^+$ expression within more dorsal midbrain regions representing non-DA populations (Martin et al., 2004; Skidmore et al., 2008). Thus, early *En1* expression appears to align with the majority of the $Pitx3^+$ DA domain. In contrast, the adjacent *Dbx1* microdomain corresponds to a region containing non-DA, $Pitx2^+$ neurons.

Intersectional and dual recombinase fate maps reveal that the mdFP is subdivided by adjacent En1 and Dbx1 microdomains with minimal developmental overlap

En1 and Dbx1 appear to mark non-overlapping regions of the mdFP. We next investigated (1) whether the En1 and Dbx1 microdomains in this specific region abut, forming a novel floor plate boundary; (2) whether there is any overlap of En1 and Dbx1 expression within progenitor cells of the mdFP at any time during early development; and (3) whether, if such overlapping cells are identified, they represent specific and novel subsets of DA neurons.

Development (2017) 144, 916-927 doi:10.1242/dev.144949

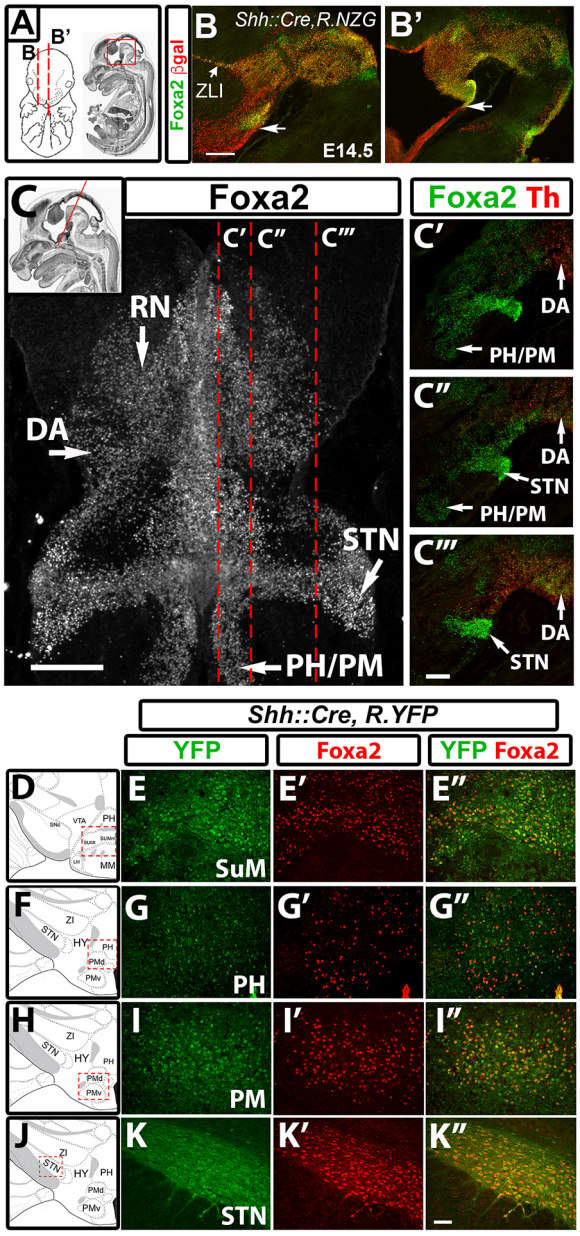

Fig. 1. DA neuron production is restricted within the Shh^{+}/Foxa2^{+} mdFP along the A-P axis. (A) Schematics of an E14.5 embryo (taken from emouseatlas.org and Allen Brain Atlas) with plane of sections shown in B,B′ indicated. (B,B′) The Foxa2^{+} domain is restricted within the broader *Shh::Cre, RC::NZG* domain (βgal) along the A-P axis (large arrows indicate anterior end of the Foxa2 domain). (C-C‴) Foxa2 immunolabeling reveals the developing DA RN populations, and apparent tangential migration of STN, PH and PM populations. Inset: schematic depicting plane of section. Dashed red lines represent sagittal planes depicted in C′-C‴, labeled with Foxa2 and Th. (D-K″) *Shh::Cre, R.YFP* P28 brain sections labeled for Foxa2 and YFP. Red dashed boxes in schematics indicate the areas shown. HY, hypothalamus; LM, lateral mammillary nucleus; MM, medial mammillary nucleus; PH, posterior hypothalamic nucleus; PMd, dorsal premammillary nucleus; PMv, ventral premammillary nucleus; SUMl, supramammillary nucleus, lateral part; SUMm, supramammillary nucleus, medial part; ZI, zona incerta. Scale bars: 200 µm (B,B′); 100 µm (C′-C‴); 50 µm (E-K″).

To answer these questions, we designed a combined intersectional and dual fate-mapping approach to label *En1* and *Dbx1* microdomains, and any overlapping regions within the same embryo. We used two recombinase drivers, *Dbx1::Cre* (Fig. S2D,D′) (Bielle et al., 2005) and *En1::Dre* (Plummer et al., 2016) in combination with two separate reporter alleles *RC::RLTG* (Rosa-CAG-rox-FRT-loxP-tdTomato-eGFP) and *RC::NZG* (Rosa-CAG-loxP-PGKNeo-FRT-nlsLacZ-eGFP) (Fig. 3A) (Plummer et al., 2015; Yamamoto et al., 2009). In such embryos, the intersectional reporter *RC::RLTG* produces expression of tdTomato after *En1::Dre* recombination, and eGFP after intersectional *En1::Dre* and *Dbx1::Cre* recombination events; *RC::NZG* expresses *nls-lacZ* after *Dbx1::Cre* recombination events. This approach allowed us to examine at improved resolution, the establishment and juxtaposition of the *En1* and *Dbx1* microdomains.

We analyzed mid-sagittal E9.5 and E11.5 sections of *En1::Dre, Dbx1::Cre, RC::RLTG, RC::NZG* embryos. Along the A-P axis of the mdFP, tdTomato^{+} cells and βgal^{+} cells form abutting microdomains with limited intermingling (Fig. 3B,C). These results demonstrate that a progenitor boundary is formed between the *En1* and *Dbx1* microdomains of the mdFP. Very few intersectionally labeled GFP^{+} cells were observed near this boundary (Fig. 3B,D; Fig. S2A). Thus, although a boundary is formed, it does not appear to involve initial overlap of *En1* and *Dbx1* transcription factors, unlike some other boundaries (Kiecker and Lumsden, 2005).

We next correlated Th expression with differentially labeled cells in these embryos. Most Th^{+} neurons were tdTomato^{+}, and further, these were aligned with the *En1*$^{+}$ progenitor microdomain, which extends up to the ZLI (Fig. 3D,D′; Fig. S3). Interestingly, a small subset of Th^{+} neurons were found outside the tdTomato-labeled microdomain, consistent with a previous study (Lahti et al., 2012) (Fig. 3D′, thick arrow). These Th^{+} cells were not GFP^{+}, and appeared to be βgal^{+}, suggesting that they were derived from the Dbx1 domain (addressed later in this article). Taken together, these data support a model wherein the *En1* microdomain of the mdFP mainly demarcates the rostral limit of DA neuron production (barring a small cohort of Th^{+} neurons), and the *Dbx1* microdomain delineates the boundary of neighboring non-DA neurons.

Other embryonic regions were also GFP^{+}, including the dorsal midbrain, hindbrain neurons located in rhombomere 1, and the spinal cord (Fig. S2A-C) (Pierani et al., 2001; Shoji et al., 1996). Indeed, GFP^{+} fibers extending from the dorsal midbrain or possibly other regions are detected in the caudal ventral midbrain (Fig. 3C,D,D″; Fig. S2A), similar to other studies reporting fibers in this region originating from the dorsal midbrain (Inamata and Shirasaki, 2014). In the spinal cord, Dbx1 and En1 expression along the D-V axis has been shown to be highly dynamic, yet partly and transiently overlapping in 5-10% of cells (Pierani et al., 1999, 2001). Our spinal cord results demonstrate that even in the case of transiently overlapping gene expression domains, our intersectional method is capable of detecting large numbers of overlapping cells, and at significantly greater sensitivity than traditional methods (Fig. S2B,C). Overall, we conclude that within the mdFP, the *En1* and *Dbx1* microdomains abut each other forming a boundary, and further, when probed at intersectional resolution, there is minimal developmental overlap.

En1, but not Dbx1, fate maps include DA and RN neurons

To fate map the *En1*$^{+}$ and *Dbx*1^{+} microdomains, we separately analyzed postnatal day (P) 28 *En1::Cre, RC::NZG* or *Dbx1::Cre, RC::NZG* animals. Analysis of *En1::Cre, RC::NZG* midbrain sections revealed Th^{+}/Foxa2^{+} substantia nigra pars compacta (SNc), ventral tegmental area (VTA), retrorubral field (RRF) and caudal linear (CLi) neurons co-labeled with βgal (Fig. 4B,E; SNc=99.3%±0.4 s.e.m., VTA=98.7%±0.2 s.e.m., RRF=99.7%±0.3 s.e.m., CLi=99.1%±0.8 s.e.m.). Th^{-}/Foxa2^{+} neurons located in the

Development (2017) 144, 916-927 doi:10.1242/dev.144949

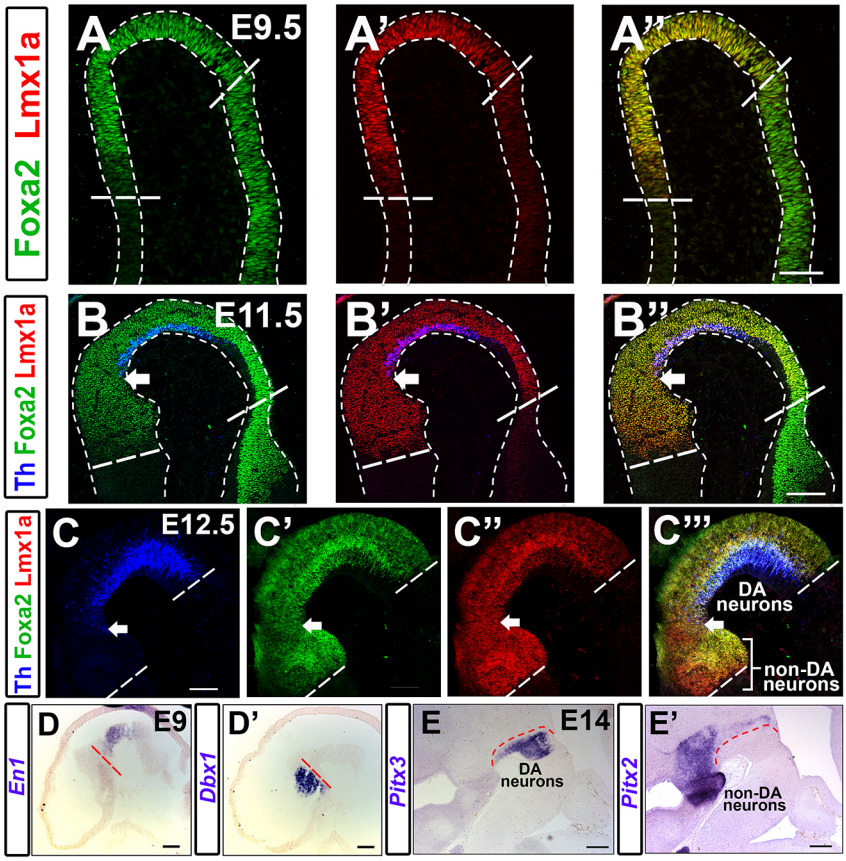

Fig. 2. Developmental expression of mdFP and postmitotic markers. (A-C‴), Developmental expression of Foxa2, Lmx1a and Th. Dashed lines demarcate the A-P extent of the mdFP. Arrows indicate rostral extent of Th^+ DA neurons. (D,D′) E9 embryos showing neighboring *En1* and *Dbx1* expression within the mdFP. (E,E′) In E14 embryos, *Pitx3*$^+$ DA neurons appear in a region adjacent to *Pitx2*$^+$ non-DA neurons (dashed red line). Some Pitx2 expression is also observed in more dorsolateral midbrain regions. Scale bars: 50 µm (A-A″); 100 µm (B-D′); 200 µm (E,E′).

rostral linear (RLi) region were also co-labeled with βgal (not shown). βgal was also observed in $Pou4f1^+/Foxa2^+$ cells of the RN in *En1::Cre, RC::NZG* fate maps (Fig. S3B-C′). Indeed, in sagittal embryonic sections, $βgal^+/Foxa2^+/Pou4f1^+$ cells were observed throughout the midbrain with a rostral limit near the ZLI, similar to Th^+ DA neurons (Fig. S3A-B‴).

In *Dbx1::Cre, RC::NZG* fate maps, βgal did not colocalize with $Th^+/Foxa2^+$ DA neurons of the VTA, SNc, RRF or CLi (Fig. 4C,F; data not shown). Also, cells in the RLi region were $βgal^-$ (data not shown). $βgal^+$ cells also did not co-label with $Pou4f1^+/Foxa2^+$ RN neurons (data not shown). Finally, $βgal^+/Th^-$ cells were also observed in the vicinity of DA neurons in both En1 and Dbx1 fate maps (Fig. 4B,C,E,F, arrowheads). As these cells are $Foxa2^-$, they could potentially represent interneurons that have migrated from more dorsal regions and/or the hindbrain (Lahti et al., 2016). In summary, *En1*$^+$ but not *Dbx1*$^+$ mdFP derivatives include DA, RN and RLi neurons. The few *Dbx1* microdomain-derived Th^+ neurons observed in Fig. 3D,D′, do not contribute to the SNc and VTA, and probably contribute to scattered Th^+ neurons in the hypothalamic region.

The Dbx1$^+$ mdFP microdomain gives rise to hypothalamic neurons

En1 and *Dbx1* single fate-mapping analyses were also used to determine the origin of neighboring hypothalamic populations. The glutamatergic STN is a hypothalamic population just rostral to the SNc, which has been shown to express Pitx2 (Fig. 5A-C) (Martin et al., 2004; Skidmore et al., 2008, 2012). Interestingly, we determined that the STN maintains expression of the floor plate markers Foxa2 and Lmx1a, but is negative for βgal in *En1::Cre, RC::NZG* fate maps (Fig. 5A,D,F). In contrast, *Dbx1::Cre, RC::NZG* fate maps show βgal colocalized with all $Pitx2^+$, $Foxa2^+$ and $Lmx1a^+$ cells of the STN and parasubthalamic nucleus (PSTN) (Fig. 5A,C,E,G; data not shown for PSTN). Additionally, the STN and PSTN also express Nr4a2, an important marker of FP-derived DA neurons (data not shown).

Further analysis revealed robust expression of the mdFP markers Foxa2 and Lmx1a in more ventral medial nuclei of the PH, SuM and PM regions. The $Foxa2^+$ and $Lmx1a^+$ PH/PM neurons co-labeled with βgal in *Dbx1::Cre, RC::NZG* [Fig. 5A,I,K shows the ventral premammillary (PMv) region; PH and SuM not shown], but not in *En1::Cre, RC::NZG* fate maps (Fig. 5A,H,J). The $Foxa2^-/Lmx1a^-$ mammillary and lateral hypothalamic area were also labeled with βgal in *Dbx1::Cre, RC::NZG*, but not in *En1::Cre, RC::NZG* fate maps (data not shown). In summary, our fate maps show that two clear and non-overlapping microdomains defined by *En1* and *Dbx1* exist within the mdFP, and these give rise to distinct neuronal populations.

Ventral premammillary neurons express multiple DA neuron markers

Through separate studies in our laboratory, we identified an *Slc6a3*$^+$ population in the PMv region. To explore the possibility that this unique population expressing DA markers was derived from the mdFP, we analyzed *Slc6a3::Cre, Ai9* P30 brains. Our experiments revealed $tdTomato^+$ neurons (Fig. 6A,B) co-labeled with the markers Foxa2, Lmx1a and Nr4a2, indicative of their mdFP origin (Fig. 6C). Very few $tdTomato^+$ neurons were co-labeled with Th antibodies (Fig. 6C; zero to two neurons per section). Allen Brain Atlas (ABA) characterizations also revealed robust transcript expression of *Slc6a3*, *Ddc* and *Slc18a2* in the PMv. Although we were able to detect robust Ddc immunolabeling, we were unable to detect Slc6a3 and Slc18a2 protein in PMv cells (Fig. S5). Taken together, these analyses reveal

Development (2017) 144, 916-927 doi:10.1242/dev.144949

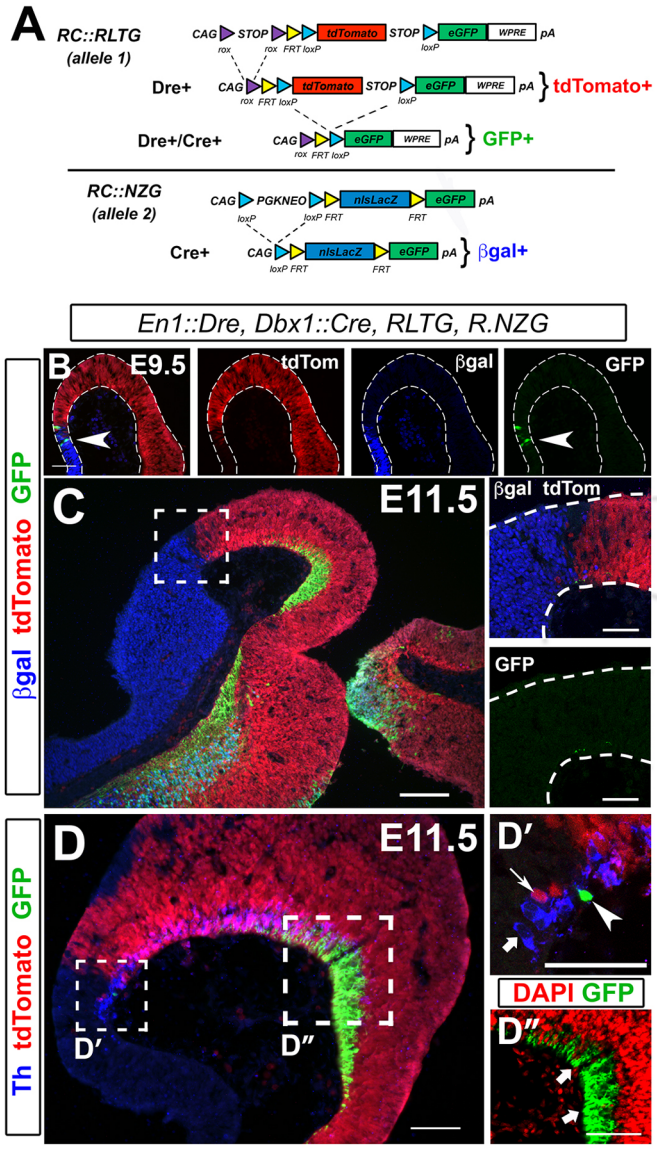

Fig. 3. Intersectional and simultaneous dual recombinase-mediated labeling of mdFP reveal abutting but minimally overlapping microdomains. (A) Schematic of *RC::RLTG* and *RC::NZG* reporters. (B,C) E9.5 and 11.5 embryos revealing adjacent microdomains (βgal and tdTomato) with little intersectional overlap (GFP$^+$ cells). Few GFP$^+$ cells are also observed in the midbrain basal plate (data not shown). (D-D″) Th$^+$ neurons are largely tdTomato$^+$. (D′) Thick arrow indicates a few Th$^+$/tdTomato$^-$ neurons. Occasional GFP$^+$ cells are observed (arrowhead). Some tdTomato$^+$ cells intermingle in the adjacent domain (thin arrow). (D″) DAPI and GFP labeling is mutually exclusive in fiber tracts derived from other intersectionally labeled populations, and therefore irrelevant to mdFP boundaries (also see Fig. S2). Arrows indicate GFP$^+$/DAPI$^-$ fibers. *n*=4. Scale bars: 50 µm (B); 100 µm (C); 50 µm (D′,D″, high magnification panels in C).

for the first time a *Dbx1*$^+$ mdFP-derived neuronal population that is positive for many key DA pathway markers, although some are detectable only at the transcript level.

Ectopic En1 expression results in significant DA neuron production from the Dbx1$^+$ mdFP

We next sought to examine if En1 expression was sufficient to generate DA neurons from the *Dbx1* microdomain. We therefore generated conditional En1 overexpressor (En1OE) mice, also designed to co-express nuclear eGFP (Fig. 7A). We inserted a

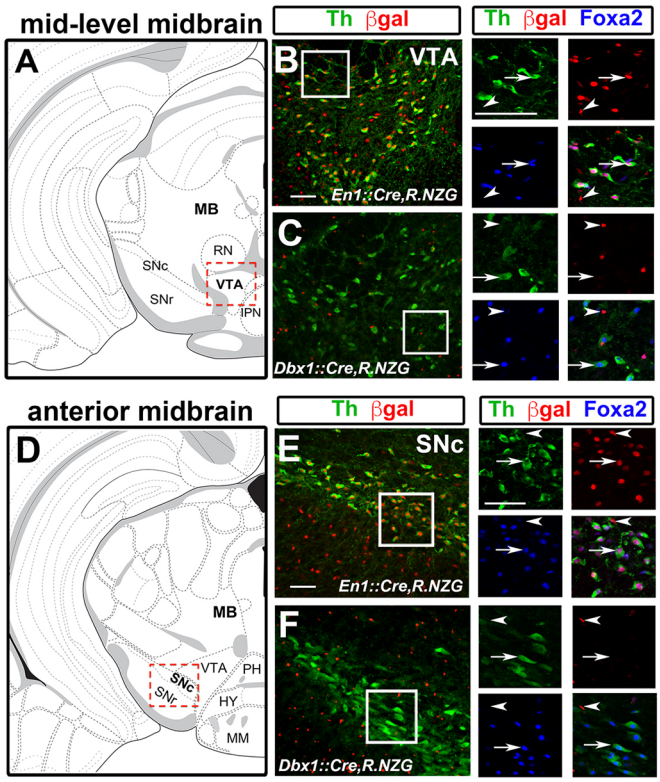

Fig. 4. En1, but not Dbx1 fate maps label VTA and SNc DA neurons. (A,D) Allen Brain Atlas schematics showing regions of interest. (B,E) *En1::Cre, RC::NZG* sections depicting Th$^+$, βgal$^+$ and Foxa2$^+$ VTA and SNc neurons. High magnification images of the boxed areas reveal co-labeled cells (arrows). Arrowheads indicate βgal$^+$, Th$^-$, Foxa2$^-$ non-DA cells. (C,F) *Dbx1::Cre, RC::NZG* sections depicting Th$^+$/Foxa2$^+$/βgal$^-$ cells in the VTA and SNc (arrows). Some βgal$^+$ non-DA cells are observed (arrowheads). *n*=3 each. HY, hypothalamus; IPN, interpeduncular nucleus; MB, midbrain; MM, medial mammillary nucleus; SNr, substantia nigra pars reticulata. Scale bars: 50 µm (B-F).

single copy of the transgene using ΦC31 integrase and attPx3 docking sites at the *Rosa26* locus (Tasic et al., 2011). We first validated conditional expression of both En1 and GFP in *Dbx1::Cre, En1OE* mutants at E10.5 (Fig. 7B-E). By this embryonic stage in controls, En1 expression appears retracted and is mainly detectable in the caudal midbrain and rostral hindbrain (Fig. 7E, arrowhead). In mutants, ectopic En1$^+$ cells were observed in the *Dbx1*$^+$ mdFP, and they also expressed eGFP (Fig. 7C, arrow), whereas En1 expression in the midbrain and hindbrain appeared normal in mutants compared with control samples (Fig. 7C-E, arrowheads). In mutant embryos, ectopic En1 appeared of comparable or slightly lower intensity to En1 expression near the MHB (Fig. 7D, arrow versus arrowhead). In addition, other CNS regions expressing Dbx1, including the dorsal midbrain and hindbrain, also co-expressed eGFP and En1 (Fig. 7B). These results suggest that our overexpressor line expresses En1 and eGFP, and that ectopic En1 levels are within a physiological range.

Next, we compared Th expression in *Dbx1::Cre, En1OE* mutants with both *Dbx1::Cre, RC::NZG* and *En1::Cre, RC::NZG* controls at E12.5. Our initial findings reveal that in controls, a few Th$^+$ neurons are observed outside the En1 and within the Dbx1 microdomain. In En1OE mutants, there appeared to be a significant rostral expansion of Th$^+$ neurons within the Foxa2 domain (Fig. 7F-I, brackets). We then analyzed Th expression at E14.5, the time point after normal DA neuron production is complete. We used coronal sections to visualize cell distributions and their boundaries better. A small

Development (2017) 144, 916-927 doi:10.1242/dev.144949

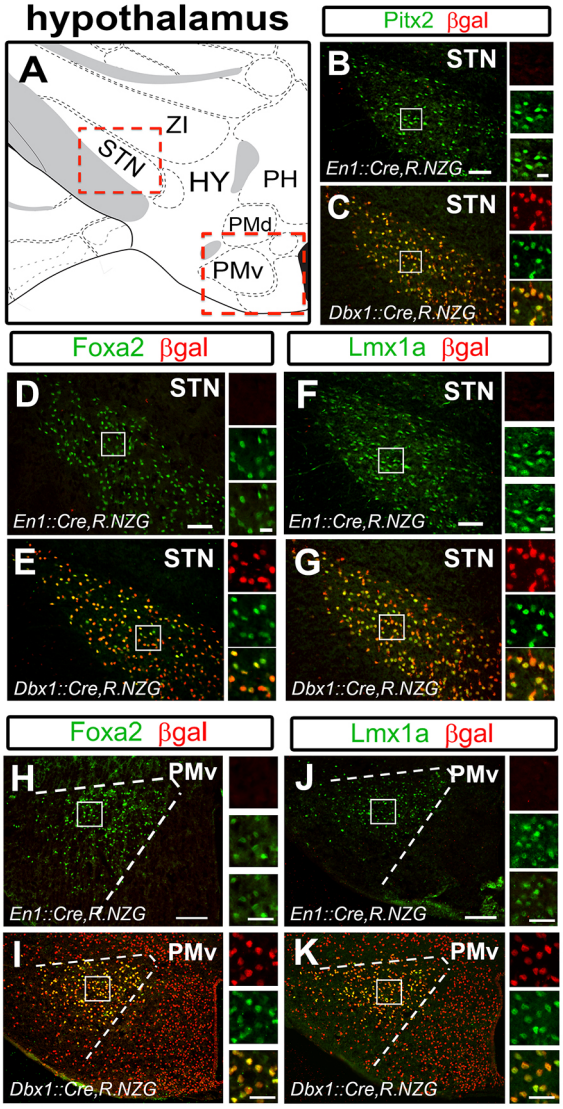

Fig. 5. Dbx1, but not En1 fate maps label STN and PM neurons. (A) Allen Brain Atlas schematic showing regions of interest. (B-K) P28 *En1::Cre, RC::NZG* and *Dbx1::Cre, RC::NZG* sections labeled with Pitx2, Foxa2, Lmx1a and βgal antibodies. STN and PMv regions are depicted. High magnification images of the boxed areas are shown separately and merged. Note that images in B,F (*En1::Cre, RC::NZG*) and C,G (*Dbx1::Cre, RC::NZG*) were obtained from the same section triple immunolabeled for Pitx2, Lmx1a and βgal, and pseudocolored to depict colocalization. *n*=6 for each antibody combination. HY, hypothalamus; PMd, dorsal premammillary nucleus; PMv, ventral premammillary nucleus; ZI, zona incerta. Scale bars: 50 µm (B-G); 100 µm (H-K).

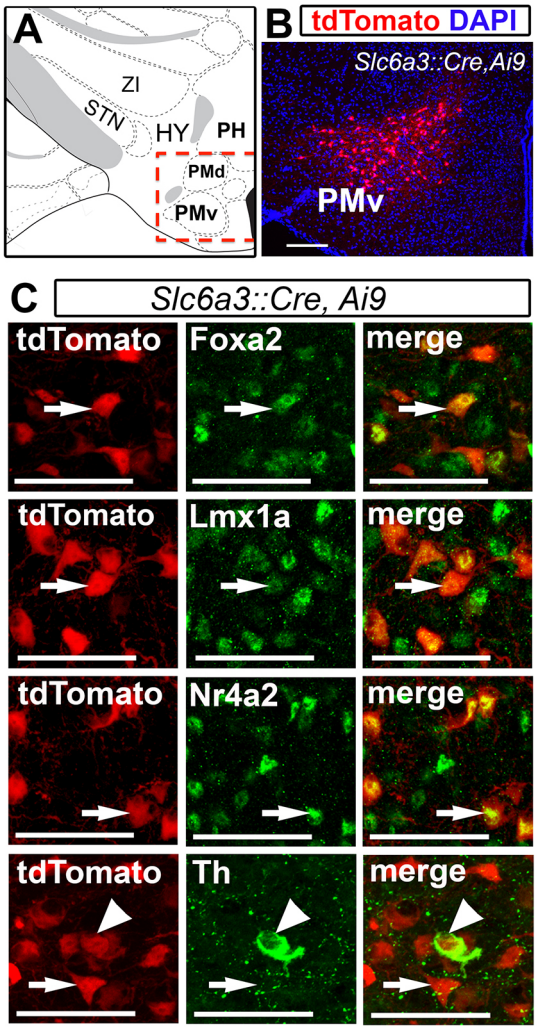

Fig. 6. DA neuron markers are expressed in ventral premammillary neurons. (A) Allen Brain Atlas schematic showing regions of interest. (B,C) P30 *Slc6a3::Cre, Ai9* sections immunolabeled with DA markers Foxa2, Lmx1a, Nr4a2 and Th (arrows indicate co-labeled cells). Only few PMv neurons (up to two per section) were Th^+ (arrowheads). HY, hypothalamus; PMd, dorsal premammillary nucleus; PMv, ventral premammillary nucleus; ZI, zona incerta. Scale bars:100 µm (B); 25 µm (C).

number of low Th^+/$Lmx1a^+$-expressing neurons can be detected in the $Dbx1^+$ mdFP region of controls, but these do not contribute to the SNc and VTA (Fig. 3; Fig. 4; Fig. 7H,I; Fig. 8A,A′). Quantitative analysis revealed a large increase of Th^+/$Lmx1a^+$ neurons in *Dbx1::Cre, En1OE* mutants in comparison with controls (Fig. 8A,A′,C,C′, G). Similar analysis for the highly specific DA marker Pitx3 revealed a highly significant increase of $Pitx3^+$ neurons (Fig. 8E,F,H) derived from the $Dbx1^+$ mdFP. We also observed ectopic Ddc and Slc18a2 immunopositive cells in this region, but very few of these expressed detectable Slc6a3 (Fig. 8B,D; Fig. S4). However, Slc6a3 is not a pan-DA marker, and it is possible the ectopic DA neurons have a molecular profile resembling a DA subset containing undetectable levels of Slc6a3 (Lammel et al., 2008).

Owing to the non-viability of postnatal *Dbx1::Cre, En1OE* mutants, we could only continue our analysis until E18.5/P0 to determine where ectopic DA neurons settle. Our analysis in *Dbx1::Cre, RC::NZG* controls revealed few Th^+/$βgal^+$ neurons, with no Pitx3 expression in the caudal hypothalamus (Fig. 9A-C, arrow). Some Th^+ axons from more caudal DA neurons projecting through this region were observed (Fig. 9B,C). Comparable sections in *Dbx1::Cre, En1OE* mutants revealed a significant number of ectopic $Pitx3^+$/Th^+ neurons (Fig. 9E,F, arrows), and many $Pitx3^+$/Th^- neurons (Fig. 9F, arrowhead). These neurons are not clustered, but rather are found scattered in the mammillary and caudal hypothalamic regions (Fig. 9D-F). Our experiments reveal that extending early En1 expression into more rostral progenitors of the Dbx1 microdomain results in significant numbers of ectopic DA neurons.

En1 misexpression in the Dbx1 microdomain causes a significant reduction in the number of STN and PM neurons

We next determined the effects of En1 overexpression on caudal hypothalamic nuclei derived from the $Dbx1^+$ mdFP. In the STN/

Development (2017) 144, 916-927 doi:10.1242/dev.144949

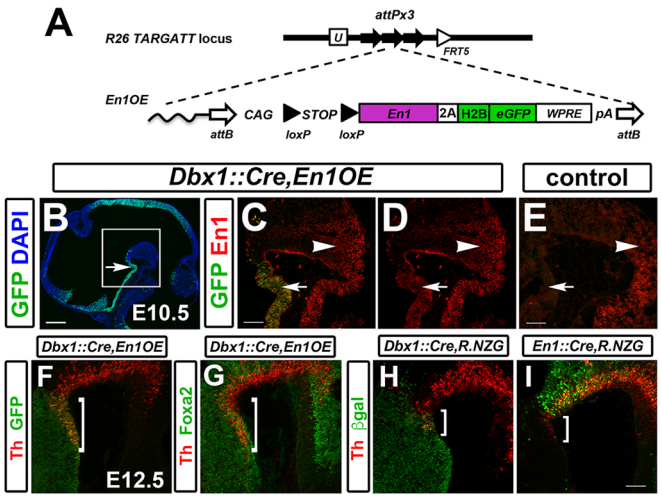

Fig. 7. Generation and validation of an En1OE knock-in mouse strain. (A) Schematic of *En1OE* construct and *Rosa26* TARGATT locus. U indicates unique sequence. (B-E) E10.5 *Dbx1::Cre, En1OE* mutant embryos, but not controls, co-express En1 and GFP in the Dbx1^{+} mdFP (arrows). Ectopic En1 levels appear to be comparable, or slightly lower than, native En1 expression in the caudal midbrain (arrows versus arrowheads in D). Panels C-E are high magnification images of the boxed area in B. (F-I) E12.5 *Dbx1::Cre, En1OE* mutants and controls co-labeled for Th with either a reporter (βgal or GFP) or Foxa2. Long bracket in F,G demarcates the expansion of Th^{+} neurons derived from the Dbx1^{+} microdomain. *n*=3 each. Scale bars: 200 µm (B); 100 µm (C-E); 50 µm (F-I).

PSTN of *Dbx1::Cre, En1OE* mutants, we observed a ∼75% reduction in the number of Pitx2^{+}/Foxa2^{+} neurons (Fig. 10A-E) compared with controls. Likewise, in the PM region of *Dbx1::Cre, En1OE* mutants, we observed an ∼85% loss of Foxa2^{+} neurons in comparison with controls (Fig. 10F-J). Very few, if any, Pitx2^{+} cells were observed in mutants. Thus, in En1OE mutants, ectopic DA neurons appear to be generated, in part, at the expense of STN and PM neurons.

DISCUSSION

Previous studies have demonstrated that the mdFP is the source of many neuron types, unlike the caudal FP, which is largely non-neurogenic. How mdFP progenitors are apportioned along the A-P axis has not been clearly elucidated. Here, we reveal (1) two microdomains, defined by En1 and Dbx1, which subdivide early FP progenitors along the A-P axis; (2) that these microdomains abut each other, with no developmental overlap and that boundary establishment is remarkably precise; (3) that an *En1*$^{+}$ microdomain gives rise to DA, RLi and RN neurons and that a *Dbx1*$^{+}$ microdomain gives rise to STN, PH, PM and SuM neurons; (4) that a subpopulation of mdFP-derived neurons express several DA-related markers within the PMv; (5) that forced expression of En1 in the *Dbx1* microdomain results in ectopic DA neurons at the expense of significant numbers of STN and PM neurons (Fig. 11). These studies are a step forward in the long-standing quest to elucidate the progenitor domains of the embryonic CNS. Furthermore, these studies will also serve as a foundation for optimizing FP-based protocols to derive DA neurons from stem cells.

Morphogens and homeodomain (HD) transcription factors are essential for the patterning and segmentation of the developing CNS (Dasen and Jessell, 2009; Kiecker and Lumsden, 2005). It has been proposed that via induction of transcription factors, morphogens define the regionalization of the CNS into distinct populations of progenitor cells with partially overlapping or 'fuzzy' expression

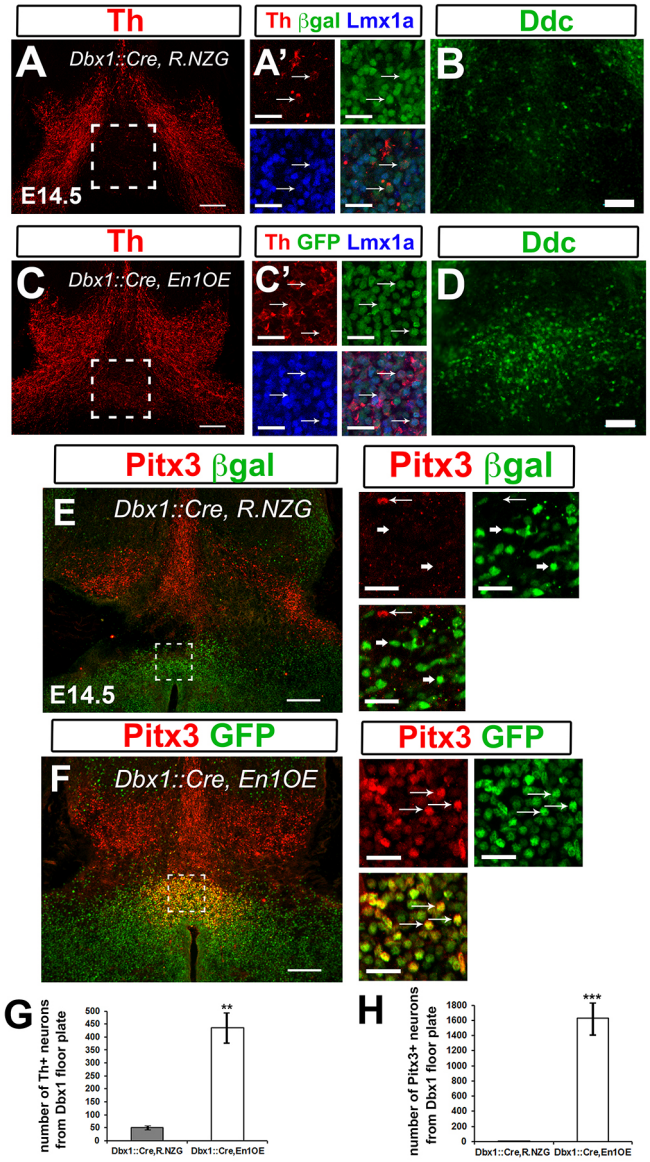

Fig. 8. Ectopic En1 expression results in DA neuron production from the Dbx1^{+} mdFP. (A-D) Coronal sections of *Dbx1::Cre, RC::NZG* controls and *Dbx1::Cre, En1OE* mutants immunolabeled with Th, Lmx1a, reporter (βgal or GFP) and Ddc (see Fig. 1C inset for plane of section). (A-B) In controls, few co-labeled cells are observed (arrows in A′), with limited Ddc expression. A′ and B are high magnification images of the boxed area in A. (C-D) In mutants, many neurons are co-labeled for Th, GFP and Lmx1a (arrows in C′) with robust ectopic Ddc expression in this region. C′ and D are high magnification images of the boxed area in C. (E) In controls, neurons in this region are Pitx3^{-}/βgal^{+} (thick arrows). An occasional nearby Pitx3^{+}/βgal^{-} neuron is observed (thin arrows). (F) In mutants, Pitx3^{+}/GFP^{+} neurons are detected (thin arrows). In E and F, high magnification images of the boxed regions are shown to the right. (G,H) Quantification of ectopic Th^{+} and Pitx3^{+} neurons in every third section. Th: *n*=3, ***P*<0.01; Pitx3: *n*=3, ****P*<0.001. Data are mean±s.e.m. Scale bars: 200 µm (A,C,E,F); 50 µm (B,D); 20 µm (high magnification panels).

boundaries that are later sharpened through cross-repressive interactions (Briscoe and Small, 2015; Kiecker and Lumsden, 2005; Prochiantz and Di Nardo, 2015). In contrast to these models of cross-repressive transcription factor interactions, here we probed boundary formation with intersectional resolution to show that this boundary forms in a remarkably precise manner, with minimal developmental overlap between the two microdomains. How this boundary forms with this remarkable level of precision

Development (2017) 144, 916-927 doi:10.1242/dev.144949

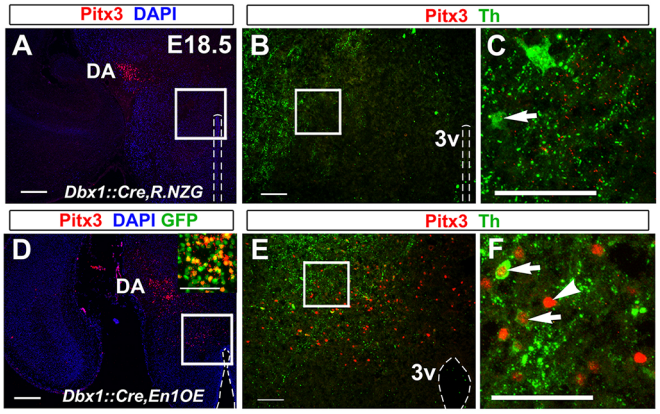

Fig. 9. Ectopic DA neurons settle in the mammillary and caudal hypothalamic areas. (A) In the control section depicted, only SNc DA neurons are Pitx3^{+}. (B,C) Few hypothalamic areas are labeled for Th, and do not express Pitx3 (arrow in C). (D-F) In mutants, ectopic Pitx3^{+}/Th^{+} and Pitx3^{+}/Th^{-} neurons are observed in hypothalamic areas (arrowhead and arrows in F). Inset in D shows that Pitx3^{+} neurons are GFP^{+}. Boxes indicate the areas shown at higher magnification on the right. 3v, third ventricle. *n*=3 each. Scale bars: 200 µm (A,B,D,E); 50 µm (C,F and inset).

remains to be determined, but one possibility could be through morphogen-induced cross-inhibitory positive-feedback mechanisms (Srinivasan et al., 2014). Differential cell-adhesion has also been invoked as a mechanism for boundary formation, and could play a role (Kiecker and Lumsden, 2005). Finally, the presence of physical barriers (e.g. extracellular matrix) could also contribute to the precision of boundary formation (Kiecker and Lumsden, 2005). Further experiments will be needed to elucidate the exact mechanism underpinning the precise formation of this boundary.

Our study reveals a subdivision of the floor plate along the A-P axis into two juxtaposed microdomains, giving rise to neighboring neuronal lineages. Based on our own analysis and results from other groups, it is clear that a multitude of early factors, which are required for DA progenitor specification, are expressed on either side of this boundary along the A-P axis. Thus, in a sense, we view these neighboring cell populations and their descendent lineages as developmental 'cousins'. We were able to identify several neuronal populations originating from either side of this boundary. The En1 microdomain gave rise to the VTA, SNc and RLi and non-dopaminergic RN neurons. The *Dbx1* microdomain did not give rise to DA neurons in the SNc and VTA, and instead gave rise to tangentially migrating neurons that contribute to the STN, PH and PM. Our data thus provides an account of mdFP descendants and refines previous models (Björklund and Dunnett, 2007; Bodea and Blaess, 2015; Puelles and Rubenstein, 2015; Smits et al., 2006; Veenvliet and Smidt, 2014) in that we demonstrate that SNc and VTA DA neuron populations are not derived from the domain rostral to the ZLI (presumptive Dbx1^{+}/Foxa2^{+} in p3 domain).

Our study identified mdFP-derived neuronal populations in the PMv that express key DA transcription factors and DA synthesis markers. PMv neurons have significant enrichment of ribosome-associated mRNAs for *Slc6a3*, *Th* and *Ddc* (Soden et al., 2016). However, levels of *Th* were 10% of those in VTA neurons. Previous studies have reported these neurons to be catecholamine immunoreactive in some circumstances (Zoli et al., 1993). Our study shows that this population of neurons is derived from the mdFP, expresses key transcription factors including Foxa2, Lmx1a

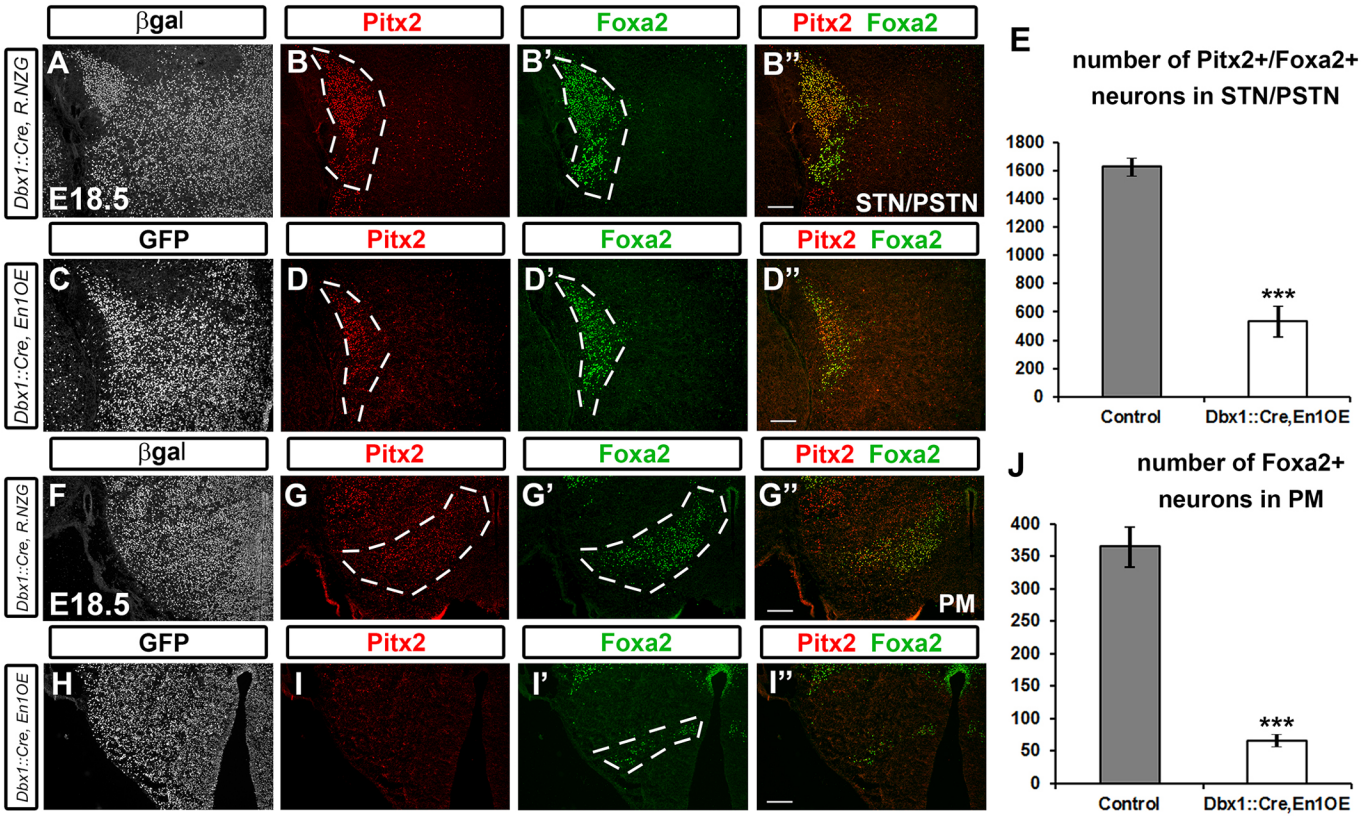

Fig. 10. Significant reduction of STN and PM neurons is observed in En1OE brains. (A-J) In mutants, compared with controls, Foxa2^{+}/Pitx2^{+} neurons are substantially reduced in the STN/PSTN (outlined; A-E) (***P<0.001; n=3 each) and in the PM (outlined; F-J) (***P<0.001; n=3 each). Data are mean±s.e.m. Scale bars: 200 µm.

Development (2017) 144, 916-927 doi:10.1242/dev.144949

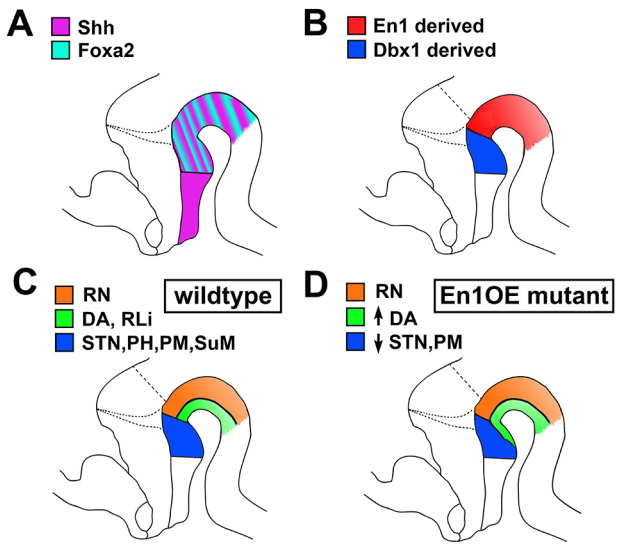

Fig. 11. Model of progenitor microdomains and their derivatives. (A-D) Mid-sagittal schematic of embryo. The ZLI (dotted outline) is located in more lateral sections. (A) Overlap of Shh and Foxa2 expression. (B) En1- and Dbx1-derived microdomains form a boundary within the mdFP. Dashed straight line represents the En1 domain in more dorsolateral regions. (C) In controls, the En1 microdomain gives rise to RN, DA and RLi neurons. The Dbx1 microdomain gives rise to STN, PM, PH and SuM neurons. (D) In *En1OE* mutants, ectopic DA neurons are produced from the Dbx1 microdomain, at the expense of STN and PM neurons.

and Nr4a2 and yet are still distinct from DA neurons in that PMv neurons are derived from the *Dbx1* microdomain, do not express *En1* or Pitx3, and only few of these cells express Th (Figs 5, 6). The lack of En1 or Pitx3 could in part account for the low levels of *Th* observed in this population, despite the presence of Nr4a2 and Foxa2, known drivers of *Th* expression (Kadkhodaei et al., 2009; Kim et al., 2003; Pristerà et al., 2015; Stott et al., 2013; Yi et al., 2014). In accordance with this, *En1* and *Pitx3* have been shown to be upstream of *Th*, and Pitx3 has been shown to potentiate the action of Nr4a2 on the *Th* promoter by releasing SMRT/HDAC-mediated repression (Jacobs et al., 2009; Veenvliet et al., 2013). Although this population expresses low levels of *Th*, there still remains the possibility that PMv neurons might have some DA-synthesis capacity under specific environmental or physiological conditions.

Embryonic loss of En1 leads to an early reduction of rostral DA neurons. Interestingly, gene expression profiling of these mutants reveals the upregulation of the marker *Pitx2* (Veenvliet et al., 2013). Utilizing a conditional overexpressor mouse model, our data reveals that En1 is sufficient to expand DA production into the *Dbx1*$^+$ mdFP, partly at the expense of STN and PM neurons. In this regard, to our knowledge this is the first study to produce an anterior expansion of Pitx3$^+$/Th$^+$ DA neurons beyond their normal expression domain. Ectopic DA neurons do not settle in the STN or PH/PM probably because they do not have the appropriate molecular profile for migration into these regions. Although the expansion of DA neurons is robust, clearly there are still some STN (~25%) and PM (~15%) neurons produced. Thus, a key question arises – why is the entire *Dbx1*$^+$ mdFP not reprogrammed to generate Th$^+$/Pitx3$^+$ DA neurons in our En1OE model? Multiple possible explanations exist, such as the lower concentration, or absence, of Fgf8 in more rostral mdFP regions, due to its distance from the MHB source. Another possibility is the lack of a complete repertoire of transcription factors in subregions of the *Dbx1* domain, or the presence of repressive factors in this region that preclude DA specification, and cannot be overridden by En1 alone. Finally, it is possible that our transgenic overexpression of En1 is at modest levels during early specification and is insufficient for complete reprogramming. Many studies on boundaries use electroporation, whereby higher levels can be achieved to overexpress transcription factors (Dasen et al., 2003; Matsunaga et al., 2000). When single-copy *Rosa26*-targeted transgenic approaches have been used, the results are sometimes more moderate. In the case of the MHB, when a transgenic approach was used to overexpress the key transcription factor Otx2 in r1, the MHB boundary shift was only moderate and transient (Omodei et al., 2008). Thus, it is possible that in our En1OE model, modest expression levels achieved in the early embryo were not sufficient for complete reprogramming of the *Dbx1*$^+$ mdFP to DA neurons.

Recent advances in the generation of DA neurons from stem cells have shown promising results towards potential cell replacement therapies and modeling studies for Parkinson's disease (Cooper et al., 2012; Grealish et al., 2014; Kirkeby et al., 2012; Kriks et al., 2011; Mazzulli et al., 2016; Xi et al., 2012). Key protocols designed for the conversion of induced pluripotent stem cells (iPSCs) into DA neurons were based on previous developmental studies showing DA neurons arise from FP progenitors, and use FOXA2 and LMX1A to optimize DA neuron derivation protocols (Kirkeby et al., 2012; Kriks et al., 2011; Xi et al., 2012). However, immunolabeling studies on cultured and grafted DA neurons show that many neurons in the graft are FOXA2$^+$ but not TH$^+$, probably representing a non-DA fate. Gene expression analysis of these cultures showed robust upregulation of *DBX1* and *PITX2*, in addition to DA markers (Kriks et al., 2011; Xia et al., 2016), indicative of imperfect programming. As these protocols were designed to maximize FOXA2$^+$/LMX1A$^+$ progenitor cells, our work would predict that both DBX1 and EN1 progenitors were generated, consequently resulting in the differentiation of DA and non-DA neurons. Specifically detailing the exact microdomains within the mdFP *in vivo* presents an exciting advance towards designing protocols for more homogeneous and efficient production of DA neurons from iPSCs. Achieving large fractions of authentic DA progenitors will open up the possibility of generating and characterizing molecularly distinct DA subtypes (Anderegg et al., 2015; Poulin et al., 2014), an important goal for understanding selective DA neuron vulnerability.

MATERIALS AND METHODS

Mouse strains

Mice were maintained and sacrificed according to protocols approved by the Northwestern University Animal Care and Use Committee (IACUC). Strains include *En1::Cre* (Kimmel et al., 2000), *En1::Dre* (Plummer et al., 2016), *Dbx1::Cre* (Bielle et al., 2005), *Shh::Cre* (Harfe et al., 2004), *Slc6a3::Cre* (Bäckman et al., 2006), *RC::NZG* (Yamamoto et al., 2009), *RC::RLTG* (Plummer et al., 2015), *RC::YFP* (Srinivas et al., 2001) and *Ai9* (Madisen et al., 2010). For simultaneous dual and intersectional fate mapping, *En1::Dre, RC::NZG* males were bred to *Dbx1::Cre, RC::RLTG* females. Male mice could not be used carrying both *Dbx1::Cre* and reporter alleles, due to the early activation of *Dbx1::Cre*. In the case of *En1::Dre*, only occasional embryos displayed germline recombination, and these were not further analyzed.

Generation of En1OE mouse line

To generate the *En1OE* transgene, plasmid *Ai9* (Addgene, 22799) was subcloned into *pBT378* (Addgene, 52554). A plasmid *pCS2-TAG* (Addgene, 26772) was amplified for the *2A-H2B-eGFP* sequence and mouse *En1ORF* plasmid (GE-Dharmacon, OMM5895-202525739) was amplified without a stop codon. Utilizing an In-Fusion HD Cloning Kit (Clontech, 638916) linearized *pBT378/Ai9*, *En1ORF* and *2A-H2B-eGFP* were fused to obtain the final construct (5′-*attB-CAG-loxP-STOP-loxP-*

Development (2017) 144, 916-927 doi:10.1242/dev.144949

En1ORF-2A-H2B-eGFP-WPRE-bGHpA-attB-3′ with a *pBT378* backbone). The open reading frame was validated by sequencing.

Transgenic TARGATT *Rosa26(attPx3)* FVB males (Tasic et al., 2011), were crossed to wild-type C57BL/6 females. Full circular En1OE plasmid containing attB/attB sites and ΦC31 integrase mRNA was co-injected into the FVB/B6 fertilized eggs. One male founder from a total of 27 animals screened was identified for integration of the *En1OE* transgene into one *Rosa26(attPx3)* locus using primers Rosa10, 11, 425, 436 and 522 (Tasic et al., 2011), in addition to primers for WPRE and eGFP.

RNA *in situ* hybridization and immunolabeling

mRNA *in situ* hybridization was performed as previously described (Caronia-Brown et al., 2016). For immunolabeling, tissue sections were processed as previously described (Nouri et al., 2015). Antibodies used were guinea-pig anti-Lmx1a (Yong Chao-Ma, Northwestern University, Evanston, IL, USA; 1:20,000), rabbit anti-Lmx1a (Millipore, AB10533; 1:1000), goat anti-Foxa2 (Santa Cruz, SC6554; 1:50), mouse anti-Pou4f1 (Santa Cruz, sc-31984; 1:50), rabbit and sheep anti-Th (Pel-Freeze, P40101-0/P60101-150; 1:500), mouse anti-Th (Sigma, T2928; 1:1000), mouse anti-En1 (DSHB, 4G11; 1:50), chicken anti-GFP (Abcam, ab13970; 1:1500 or 1:20,000), goat anti-βgal (Biogenesis, 4600-1409; 1:1500), rabbit anti-βgal (Cappel, 55976; 1:1500), rabbit anti-Nr4a2 (Santa Cruz, SC-991; 1:50), rabbit anti-Pitx2 (Capra Science, PA 1020-100; 1:1000), rabbit anti-Pitx3 (Invitrogen/Zymed, 38-2850; 1:200), rat anti-Slc6a3 (Santa Cruz, sc-32258; 1:50), rabbit anti-Ddc (Abcam, ab3905; 1:500) and rabbit anti-Slc18a2 (EMD Millipore, AB1598P; 1:500).

Statistical analysis

Quantification is shown as mean±s.e.m., using Student's two-sample *t*-test, significant differences were taken at $P \leq 0.05$. All cells were counted on every third 20 µm coronal section at E14.5 and E18.5/P0 or counted on every sixth 20 µm coronal section (Th^+ and $\beta gal^+/Th^+$ total) at 4 weeks postnatally in *En1::Cre, RC::NZG* fate maps (n=3).

Image acquisition

All images were acquired using Leica DM5000B epifluorescence, Leica TCS SP5 confocal or Nikon A1R(A) Spectral confocal microscopes. Adobe Photoshop CC 2015 was utilized for the overlay of pseudocolored single-channel images in the same sections for some figures, and to adjust brightness and contrast for all figures shown.

Note added in proof

While this paper was in revision, an interesting manuscript relevant to this topic was published (Kee et al., 2017).

Acknowledgements

We thank Dr Patricia Jensen for providing *En1::Dre* and *RC::RLTG* mice, Dr Yong Chao-Ma for Lmx1a antibodies, Nigel P. Anderson for technical help, Jean-Francois Poulin for sharing findings, and critiques on the manuscript. En1OE mice were generated by the TTML core. Imaging was performed at the Center for Advanced Microscopy (NCI-CCSG-P30-CA060553).

Competing interests

The authors declare no competing or financial interests.

Author contributions

N.N. designed and conducted experiments, prepared figures and wrote the manuscript. R.A. supervised the study and revised the manuscript.

Funding

R.A. was supported by grants from the National Institute of Neurological Disorders and Stroke (1R21NS072703-01, RO1NS096240-01) and by the National Alliance for Research on Schizophrenia and Depression. N.N. was supported by a Northwestern University Feinberg School of Medicine Center for Genetic Medicine Travel Fellowship. Deposited in PMC for release after 12 months.

Supplementary information

Supplementary information available online at
http://dev.biologists.org/lookup/doi/10.1242/dev.144949.supplemental

References

Alberi, L., Sgado, P. and Simon, H. H. (2004). Engrailed genes are cell-autonomously required to prevent apoptosis in mesencephalic dopaminergic neurons. *Development* **131**, 3229-3236.

Alvarez-Bolado, G., Paul, F. A. and Blaess, S. (2012). Sonic hedgehog lineage in the mouse hypothalamus: from progenitor domains to hypothalamic regions. *Neural Dev.* **7**, 4.

Alvarez-Fischer, D., Fuchs, J., Castagner, F., Stettler, O., Massiani-Beaudoin, O., Moya, K. L., Bouillot, C., Oertel, W. H., Lombès, A., Faigle, W. et al. (2011). Engrailed protects mouse midbrain dopaminergic neurons against mitochondrial complex I insults. *Nat. Neurosci.* **14**, 1260-1266.

Alves dos Santos, M. T. M. and Smidt, M. P. (2011). En1 and Wnt signaling in midbrain dopaminergic neuronal development. *Neural Dev.* **6**, 23.

Anderegg, A., Lin, H.-P., Chen, J.-A., Caronia-Brown, G., Cherepanova, N., Yun, B., Joksimovic, M., Rock, J., Harfe, B. D., Johnson, R. et al. (2013). An Lmx1b-miR135a2 regulatory circuit modulates Wnt1/Wnt signaling and determines the size of the midbrain dopaminergic progenitor pool. *PLoS Genet.* **9**, e1003973.

Anderegg, A., Poulin, J.-F. and Awatramani, R. (2015). Molecular heterogeneity of midbrain dopaminergic neurons–moving toward single cell resolution. *FEBS Lett.* **589**, 3714-3726.

Andersson, E., Tryggvason, U., Deng, Q., Friling, S., Alekseenko, Z., Robert, B., Perlmann, T. and Ericson, J. (2006). Identification of intrinsic determinants of midbrain dopamine neurons. *Cell* **124**, 393-405.

Arenas, E., Denham, M. and Villaescusa, J. C. (2015). How to make a midbrain dopaminergic neuron. *Development* **142**, 1918-1936.

Bäckman, C. M., Malik, N., Zhang, Y. J., Shan, L., Grinberg, A., Hoffer, B. J., Westphal, H. and Tomac, A. C. (2006). Characterization of a mouse strain expressing Cre recombinase from the 3′ untranslated region of the dopamine transporter locus. *Genesis* **44**, 383-390.

Bedont, J. L., Newman, E. A. and Blackshaw, S. (2015). Patterning, specification, and differentiation in the developing hypothalamus. *Wiley Interdiscip. Rev. Dev. Biol.* **4**, 445-468.

Bielle, F., Griveau, A., Narboux-Nême, N., Vigneau, S., Sigrist, M., Arber, S., Wassef, M. and Pierani, A. (2005). Multiple origins of Cajal-Retzius cells at the borders of the developing pallium. *Nat. Neurosci.* **8**, 1002-1012.

Björklund, A. and Dunnett, S. B. (2007). Dopamine neuron systems in the brain: an update. *Trends Neurosci.* **30**, 194-202.

Blaess, S. and Ang, S.-L. (2015). Genetic control of midbrain dopaminergic neuron development. *Wiley Interdiscip. Rev. Dev. Biol.* **4**, 113-134.

Blaess, S., Bodea, G. O., Kabanova, A., Chanet, S., Mugniery, E., Derouiche, A., Stephen, D. and Joyner, A. L. (2011). Temporal-spatial changes in Sonic Hedgehog expression and signaling reveal different potentials of ventral mesencephalic progenitors to populate distinct ventral midbrain nuclei. *Neural Dev.* **6**, 29.

Bodea, G. O. and Blaess, S. (2015). Establishing diversity in the dopaminergic system. *FEBS Lett.* **589**, 3773-3785.

Briscoe, J. and Small, S. (2015). Morphogen rules: design principles of gradient-mediated embryo patterning. *Development* **142**, 3996-4009.

Brodski, C., Weisenhorn, D. M., Signore, M., Sillaber, I., Oesterheld, M., Broccoli, V., Acampora, D., Simeone, A. and Wurst, W. (2003). Location and size of dopaminergic and serotonergic cell populations are controlled by the position of the midbrain-hindbrain organizer. *J. Neurosci.* **23**, 4199-4207.

Caronia-Brown, G., Anderegg, A. and Awatramani, R. (2016). Expression and functional analysis of the Wnt/beta-catenin induced mir-135a-2 locus in embryonic forebrain development. *Neural Dev.* **11**, 9.

Causeret, F., Ensini, M., Teissier, A., Kessaris, N., Richardson, W. D., Lucas de Couville, T. and Pierani, A. (2011). Dbx1-expressing cells are necessary for the survival of the mammalian anterior neural and craniofacial structures. *PLoS ONE* **6**, e19367.

Chi, C. L., Martinez, S., Wurst, W. and Martin, G. R. (2003). The isthmic organizer signal FGF8 is required for cell survival in the prospective midbrain and cerebellum. *Development* **130**, 2633-2644.

Cooper, O., Parmar, M. and Isacson, O. (2012). Characterization and criteria of embryonic stem and induced pluripotent stem cells for a dopamine replacement therapy. *Prog. Brain Res.* **200**, 265-276.

Dasen, J. S. and Jessell, T. M. (2009). Hox networks and the origins of motor neuron diversity. *Curr. Top. Dev. Biol.* **88**, 169-200.

Dasen, J. S., Liu, J.-P. and Jessell, T. M. (2003). Motor neuron columnar fate imposed by sequential phases of Hox-c activity. *Nature* **425**, 926-933.

Davis, C. A. and Joyner, A. L. (1988). Expression patterns of the homeo box-containing genes En-1 and En-2 and the proto-oncogene int-1 diverge during mouse development. *Genes Dev.* **2**, 1736-1744.

Deng, Q., Andersson, E., Hedlund, E., Alekseenko, Z., Coppola, E., Panman, L., Millonig, J. H., Brunet, J.-F., Ericson, J. and Perlmann, T. (2011). Specific and integrated roles of Lmx1a, Lmx1b and Phox2a in ventral midbrain development. *Development* **138**, 3399-3408.

Echelard, Y., Epstein, D. J., St-Jacques, B., Shen, L., Mohler, J., McMahon, J. A. and McMahon, A. P. (1993). Sonic hedgehog, a member of a family of putative signaling molecules, is implicated in the regulation of CNS polarity. *Cell* **75**, 1417-1430.

Ellisor, D., Rieser, C., Voelcker, B., Machan, J. T. and Zervas, M. (2012). Genetic dissection of midbrain dopamine neuron development in vivo. *Dev. Biol.* **372**, 249-262.
Fraser, S., Keynes, R. and Lumsden, A. (1990). Segmentation in the chick embryo hindbrain is defined by cell lineage restrictions. *Nature* **344**, 431-435.
Grealish, S., Diguet, E., Kirkeby, A., Mattsson, B., Heuer, A., Bramoulle, Y., Van Camp, N., Perrier, A. L., Hantraye, P., Björklund, A. et al. (2014). Human ESC-derived dopamine neurons show similar preclinical efficacy and potency to fetal neurons when grafted in a rat model of Parkinson's disease. *Cell Stem Cell* **15**, 653-665.
Harfe, B. D., Scherz, P. J., Nissim, S., Tian, H., McMahon, A. P. and Tabin, C. J. (2004). Evidence for an expansion-based temporal Shh gradient in specifying vertebrate digit identities. *Cell* **118**, 517-528.
Hayes, L., Zhang, Z., Albert, P., Zervas, M. and Ahn, S. (2011). Timing of Sonic hedgehog and Gli1 expression segregates midbrain dopamine neurons. *J. Comp. Neurol.* **519**, 3001-3018.
Inamata, Y. and Shirasaki, R. (2014). Dbx1 triggers crucial molecular programs required for midline crossing by midbrain commissural axons. *Development* **141**, 1260-1271.
Jacobs, F. M. J., van Erp, S., van der Linden, A. J. A., von Oerthel, L., Burbach, J. P. H. and Smidt, M. P. (2009). Pitx3 potentiates Nurr1 in dopamine neuron terminal differentiation through release of SMRT-mediated repression. *Development* **136**, 531-540.
Joksimovic, M. and Awatramani, R. (2014). Wnt/beta-catenin signaling in midbrain dopaminergic neuron specification and neurogenesis. *J. Mol. Cell Biol.* **6**, 27-33.
Joksimovic, M., Anderegg, A., Roy, A., Campochiaro, L., Yun, B., Kittappa, R., McKay, R. and Awatramani, R. (2009). Spatiotemporally separable Shh domains in the midbrain define distinct dopaminergic progenitor pools. *Proc. Natl. Acad. Sci. USA* **106**, 19185-19190.
Joyner, A. L., Liu, A. and Millet, S. (2000). Otx2, Gbx2 and Fgf8 interact to position and maintain a mid-hindbrain organizer. *Curr. Opin. Cell Biol.* **12**, 736-741.
Kadkhodaei, B., Ito, T., Joodmardi, E., Mattsson, B., Rouillard, C., Carta, M., Muramatsu, S.-I., Sumi-Ichinose, C., Nomura, T., Metzger, D. et al. (2009). Nurr1 is required for maintenance of maturing and adult midbrain dopamine neurons. *J. Neurosci.* **29**, 15923-15932.
Karaz, S., Courgeon, M., Lepetit, H., Bruno, E., Pannone, R., Tarallo, A., Thouzé, F., Kerner, P., Vervoort, M., Causeret, F. et al. (2016). Neuronal fate specification by the Dbx1 transcription factor is linked to the evolutionary acquisition of a novel functional domain. *Evodevo* **7**, 18.
Kee, N., Volakakis, N., Kirkeby, A., Dahl, L., Storvall, H., Nolbrant, S., Lahti, L., Bjorklund, A. K., Gillberg, L., Joodmardi, E., et al. (2017). Single-cell analysis reveals a close relationship between differentiating dopamine and subthalamic nucleus neuronal lineages. *Cell Stem Cell* **20**, 29-40.
Kiecker, C. and Lumsden, A. (2005). Compartments and their boundaries in vertebrate brain development. *Nat. Rev. Neurosci.* **6**, 553-564.
Kim, K.-S., Kim, C.-H., Hwang, D.-Y., Seo, H., Chung, S., Hong, S. J., Lim, J.-K., Anderson, T. and Isacson, O. (2003). Orphan nuclear receptor Nurr1 directly transactivates the promoter activity of the tyrosine hydroxylase gene in a cell-specific manner. *J. Neurochem.* **85**, 622-634.
Kimmel, R. A., Turnbull, D. H., Blanquet, V., Wurst, W., Loomis, C. A. and Joyner, A. L. (2000). Two lineage boundaries coordinate vertebrate apical ectodermal ridge formation. *Genes Dev.* **14**, 1377-1389.
Kirkeby, A., Grealish, S., Wolf, D. A., Nelander, J., Wood, J., Lundblad, M., Lindvall, O. and Parmar, M. (2012). Generation of regionally specified neural progenitors and functional neurons from human embryonic stem cells under defined conditions. *Cell Rep.* **1**, 703-714.
Kriks, S., Shim, J. W., Piao, J., Ganat, Y. M., Wakeman, D. R., Xie, Z., Carrillo-Reid, L., Auyeung, G., Antonacci, C., Buch, A. et al. (2011). Dopamine neurons derived from human ES cells efficiently engraft in animal models of Parkinson's disease. *Nature* **480**, 547-551.
Lahti, L., Peltopuro, P., Piepponen, T. P. and Partanen, J. (2012). Cell-autonomous FGF signaling regulates anteroposterior patterning and neuronal differentiation in the mesodiencephalic dopaminergic progenitor domain. *Development* **139**, 894-905.
Lahti, L., Haugas, M., Tikker, L., Airavaara, M., Voutilainen, M. H., Anttila, J., Kumar, S., Inkinen, C., Salminen, M. and Partanen, J. (2016). Differentiation and molecular heterogeneity of inhibitory and excitatory neurons associated with midbrain dopaminergic nuclei. *Development* **143**, 516-529.
Lammel, S., Hetzel, A., Häckel, O., Jones, I., Liss, B. and Roeper, J. (2008). Unique properties of mesoprefrontal neurons within a dual mesocorticolimbic dopamine system. *Neuron* **57**, 760-773.
Lin, W., Metzakopian, E., Mavromatakis, Y. E., Gao, N., Balaskas, N., Sasaki, H., Briscoe, J., Whitsett, J. A., Goulding, M., Kaestner, K. H. et al. (2009). Foxa1 and Foxa2 function both upstream of and cooperatively with Lmx1a and Lmx1b in a feedforward loop promoting mesodiencephalic dopaminergic neuron development. *Dev. Biol.* **333**, 386-396.
Luo, S. X. and Huang, E. J. (2016). Dopaminergic neurons and brain reward pathways: from neurogenesis to circuit assembly. *Am. J. Pathol.* **186**, 478-488.
Madisen, L., Zwingman, T. A., Sunkin, S. M., Oh, S. W., Zariwala, H. A., Gu, H., Ng, L. L., Palmiter, R. D., Hawrylycz, M. J., Jones, A. R. et al. (2010). A robust and high-throughput Cre reporting and characterization system for the whole mouse brain. *Nat. Neurosci.* **13**, 133-140.
Martin, D. M., Skidmore, J. M., Philips, S. T., Vieira, C., Gage, P. J., Condie, B. G., Raphael, Y., Martinez, S. and Camper, S. A. (2004). PITX2 is required for normal development of neurons in the mouse subthalamic nucleus and midbrain. *Dev. Biol.* **267**, 93-108.
Matsunaga, E., Araki, I. and Nakamura, H. (2000). Pax6 defines the di-mesencephalic boundary by repressing En1 and Pax2. *Development* **127**, 2357-2365.
Mazzulli, J. R., Zunke, F., Isacson, O., Studer, L. and Krainc, D. (2016). alpha-Synuclein-induced lysosomal dysfunction occurs through disruptions in protein trafficking in human midbrain synucleinopathy models. *Proc. Natl. Acad. Sci. USA* **113**, 1931-1936.
Nakatani, T., Kumai, M., Mizuhara, E., Minaki, Y. and Ono, Y. (2010). Lmx1a and Lmx1b cooperate with Foxa2 to coordinate the specification of dopaminergic neurons and control of floor plate cell differentiation in the developing mesencephalon. *Dev. Biol.* **339**, 101-113.
Nordström, U., Beauvais, G., Ghosh, A., Pulikkaparambil Sasidharan, B. C., Lundblad, M., Fuchs, J., Joshi, R. L., Lipton, J. W., Roholt, A., Medicetty, S. et al. (2015). Progressive nigrostriatal terminal dysfunction and degeneration in the engrailed1 heterozygous mouse model of Parkinson's disease. *Neurobiol. Dis.* **73**, 70-82.
Nouri, N., Patel, M. J., Joksimovic, M., Poulin, J.-F., Anderegg, A., Taketo, M. M., Ma, Y.-C. and Awatramani, R. (2015). Excessive Wnt/beta-catenin signaling promotes midbrain floor plate neurogenesis, but results in vacillating dopamine progenitors. *Mol. Cell. Neurosci.* **68**, 131-142.
Omodei, D., Acampora, D., Mancuso, P., Prakash, N., Di Giovannantonio, L. G., Wurst, W. and Simeone, A. (2008). Anterior-posterior graded response to Otx2 controls proliferation and differentiation of dopaminergic progenitors in the ventral mesencephalon. *Development* **135**, 3459-3470.
Ono, Y., Nakatani, T., Sakamoto, Y., Mizuhara, E., Minaki, Y., Kumai, M., Hamaguchi, A., Nishimura, M., Inoue, Y., Hayashi, H. et al. (2007). Differences in neurogenic potential in floor plate cells along an anteroposterior location: midbrain dopaminergic neurons originate from mesencephalic floor plate cells. *Development* **134**, 3213-3225.
Pierani, A., Brenner-Morton, S., Chiang, C. and Jessell, T. M. (1999). A sonic hedgehog-independent, retinoid-activated pathway of neurogenesis in the ventral spinal cord. *Cell* **97**, 903-915.
Pierani, A., Moran-Rivard, L., Sunshine, M. J., Littman, D. R., Goulding, M. and Jessell, T. M. (2001). Control of interneuron fate in the developing spinal cord by the progenitor homeodomain protein Dbx1. *Neuron* **29**, 367-384.
Plummer, N. W., Evsyukova, I. Y., Robertson, S. D., de Marchena, J., Tucker, C. J. and Jensen, P. (2015). Expanding the power of recombinase-based labeling to uncover cellular diversity. *Development* **142**, 4385-4393.
Plummer, N. W., de Marchena, J. and Jensen, P. (2016). A knock-in allele of En1 expressing dre recombinase. *Genesis* **54**, 447-454.
Poulin, J.-F., Zou, J., Drouin-Ouellet, J., Kim, K.-Y. A., Cicchetti, F. and Awatramani, R. B. (2014). Defining midbrain dopaminergic neuron diversity by single-cell gene expression profiling. *Cell Rep.* **9**, 930-943.
Prakash, N., Puelles, E., Freude, K., Trumbach, D., Omodei, D., Di Salvio, M., Sussel, L., Ericson, J., Sander, M., Simeone, A. et al. (2009). Nkx6-1 controls the identity and fate of red nucleus and oculomotor neurons in the mouse midbrain. *Development* **136**, 2545-2555.
Pristerà, A., Lin, W., Kaufmann, A.-K., Brimblecombe, K. R., Threlfell, S., Dodson, P. D., Magill, P. J., Fernandes, C., Cragg, S. J. and Ang, S.-L. (2015). Transcription factors FOXA1 and FOXA2 maintain dopaminergic neuronal properties and control feeding behavior in adult mice. *Proc. Natl. Acad. Sci. USA* **112**, E4929-E4938.
Prochiantz, A. and Di Nardo, A. A. (2015). Homeoprotein signaling in the developing and adult nervous system. *Neuron* **85**, 911-925.
Puelles, L. and Rubenstein, J. L. R. (2015). A new scenario of hypothalamic organization: rationale of new hypotheses introduced in the updated prosomeric model. *Front. Neuroanat.* **9**, 27.
Puelles, E., Annino, A., Tuorto, F., Usiello, A., Acampora, D., Czerny, T., Brodski, C., Ang, S.-L., Wurst, W. and Simeone, A. (2004). Otx2 regulates the extent, identity and fate of neuronal progenitor domains in the ventral midbrain. *Development* **131**, 2037-2048.
Puelles, L., Harrison, M., Paxinos, G. and Watson, C. (2013). A developmental ontology for the mammalian brain based on the prosomeric model. *Trends Neurosci.* **36**, 570-578.
Rekaik, H., Blaudin de Thé, F.-X., Fuchs, J., Massiani-Beaudoin, O., Prochiantz, A. and Joshi, R. L. (2015). Engrailed homeoprotein protects mesencephalic dopaminergic neurons from oxidative stress. *Cell Rep.* **13**, 242-250.
Rubenstein, J. L. R., Martinez, S., Shimamura, K. and Puelles, L. (1994). The embryonic vertebrate forebrain: the prosomeric model. *Science* **266**, 578-580.
Scholpp, S., Lohs, C. and Brand, M. (2003). Engrailed and Fgf8 act synergistically to maintain the boundary between diencephalon and mesencephalon. *Development* **130**, 4881-4893.

Seitanidou, T., Schneider-Maunoury, S., Desmarquet, C., Wilkinson, D. G. and Charnay, P. (1997). Krox-20 is a key regulator of rhombomere-specific gene expression in the developing hindbrain. *Mech. Dev.* **65**, 31-42.
Shimogori, T., Lee, D. A., Miranda-Angulo, A., Yang, Y., Wang, H., Jiang, L., Yoshida, A. C., Kataoka, A., Mashiko, H., Avetisyan, M. et al. (2010). A genomic atlas of mouse hypothalamic development. *Nat. Neurosci.* **13**, 767-775.
Shoji, H., Ito, T., Wakamatsu, Y., Hayasaka, N., Ohsaki, K., Oyanagi, M., Kominami, R., Kondoh, H. and Takahashi, N. (1996). Regionalized expression of the Dbx family homeobox genes in the embryonic CNS of the mouse. *Mech. Dev.* **56**, 25-39.
Simeone, A., Puelles, E. and Acampora, D. (2002). The Otx family. *Curr. Opin. Genet. Dev.* **12**, 409-415.
Simon, H. H., Saueressig, H., Wurst, W., Goulding, M. D. and O'Leary, D. D. (2001). Fate of midbrain dopaminergic neurons controlled by the engrailed genes. *J. Neurosci.* **21**, 3126-3134.
Skidmore, J. M., Cramer, J. D., Martin, J. F. and Martin, D. M. (2008). Cre fate mapping reveals lineage specific defects in neuronal migration with loss of Pitx2 function in the developing mouse hypothalamus and subthalamic nucleus. *Mol. Cell. Neurosci.* **37**, 696-707.
Skidmore, J. M., Waite, M. R., Alvarez-Bolado, G., Puelles, L. and Martin, D. M. (2012). A novel TaulacZ allele reveals a requirement for Pitx2 in formation of the mammillothalamic tract. *Genesis* **50**, 67-73.
Smidt, M. P. and Burbach, J. P. H. (2007). How to make a mesodiencephalic dopaminergic neuron. *Nat. Rev. Neurosci.* **8**, 21-32.
Smidt, M. P., van Schaick, H. S. A., Lanctot, C., Tremblay, J. J., Cox, J. J., van der Kleij, A. A. M., Wolterink, G., Drouin, J. and Burbach, J. P. H. (1997). A homeodomain gene Ptx3 has highly restricted brain expression in mesencephalic dopaminergic neurons. *Proc. Natl. Acad. Sci. USA* **94**, 13305-13310.
Smits, S. M., Burbach, J. P. H. and Smidt, M. P. (2006). Developmental origin and fate of meso-diencephalic dopamine neurons. *Prog. Neurobiol.* **78**, 1-16.
Smits, S. M., von Oerthel, L., Hoekstra, E. J., Burbach, J. P. H. and Smidt, M. P. (2013). Molecular marker differences relate to developmental position and subsets of mesodiencephalic dopaminergic neurons. *PLoS ONE* **8**, e76037.
Soden, M. E., Miller, S. M., Burgeno, L. M., Phillips, P. E. M., Hnasko, T. S. and Zweifel, L. S. (2016). Genetic isolation of hypothalamic neurons that regulate context-specific male social behavior. *Cell Rep.* **16**, 304-313.
Sokolowski, K., Tran, T., Esumi, S., Kamal, Y., Oboti, L., Lischinsky, J., Goodrich, M., Lam, A., Carter, M., Nakagawa, Y. et al. (2016). Molecular and behavioral profiling of Dbx1-derived neurons in the arcuate, lateral and ventromedial hypothalamic nuclei. *Neural Dev.* **11**, 12.
Srinivas, S., Watanabe, T., Lin, C.-S., William, C. M., Tanabe, Y., Jessell, T. M. and Costantini, F. (2001). Cre reporter strains produced by targeted insertion of EYFP and ECFP into the ROSA26 locus. *BMC Dev. Biol.* **1**, 4.
Srinivasan, S., Hu, J. S., Currle, D. S., Fung, E. S., Hayes, W. B., Lander, A. D. and Monuki, E. S. (2014). A BMP-FGF morphogen toggle switch drives the ultrasensitive expression of multiple genes in the developing forebrain. *PLoS Comput. Biol.* **10**, e1003463.
Stott, S. R. W., Metzakopian, E., Lin, W., Kaestner, K. H., Hen, R. and Ang, S.-L. (2013). Foxa1 and foxa2 are required for the maintenance of dopaminergic properties in ventral midbrain neurons at late embryonic stages. *J. Neurosci.* **33**, 8022-8034.
Studer, L. (2012). Derivation of dopaminergic neurons from pluripotent stem cells. *Prog. Brain Res.* **200**, 243-263.
Swanson, L. W. (2012). *Brain Architecture: Understanding the Basic Plan*, 2nd edn. Oxford: Oxford University Press.
Tasic, B., Hippenmeyer, S., Wang, C., Gamboa, M., Zong, H., Chen-Tsai, Y. and Luo, L. (2011). Site-specific integrase-mediated transgenesis in mice via pronuclear injection. *Proc. Natl. Acad. Sci. USA* **108**, 7902-7907.
Thompson, C. L., Ng, L., Menon, V., Martinez, S., Lee, C.-K., Glattfelder, K., Sunkin, S. M., Henry, A., Lau, C., Dang, C. et al. (2014). A high-resolution spatiotemporal atlas of gene expression of the developing mouse brain. *Neuron* **83**, 309-323.
Veenvliet, J. V. and Smidt, M. P. (2014). Molecular mechanisms of dopaminergic subset specification: fundamental aspects and clinical perspectives. *Cell. Mol. Life Sci.* **71**, 4703-4727.
Veenvliet, J. V., Dos Santos, M. T. M. A., Kouwenhoven, W. M., von Oerthel, L., Lim, J. L., van der Linden, A. J. A., Koerkamp, M. J. A. G., Holstege, F. C. P. and Smidt, M. P. (2013). Specification of dopaminergic subsets involves interplay of En1 and Pitx3. *Development* **140**, 3373-3384.
Wilkinson, D. G., Bhatt, S., Chavrier, P., Bravo, R. and Charnay, P. (1989). Segment-specific expression of a zinc-finger gene in the developing nervous system of the mouse. *Nature* **337**, 461-464.
Wurst, W. and Prakash, N. (2014). Wnt1-regulated genetic networks in midbrain dopaminergic neuron development. *J. Mol. Cell Biol.* **6**, 34-41.
Xi, J., Liu, Y., Liu, H., Chen, H., Emborg, M. E. and Zhang, S.-C. (2012). Specification of midbrain dopamine neurons from primate pluripotent stem cells. *Stem Cells* **30**, 1655-1663.
Xia, N., Zhang, P., Fang, F., Wang, Z., Rothstein, M., Angulo, B., Chiang, R., Taylor, J. and Reijo Pera, R. A. (2016). Transcriptional comparison of human induced and primary midbrain dopaminergic neurons. *Sci. Rep.* **6**, 20270.
Yamamoto, M., Shook, N. A., Kanisicak, O., Yamamoto, S., Wosczyna, M. N., Camp, J. R. and Goldhamer, D. J. (2009). A multifunctional reporter mouse line for Cre- and FLP-dependent lineage analysis. *Genesis* **47**, 107-114.
Yan, C. H., Levesque, M., Claxton, S., Johnson, R. L. and Ang, S.-L. (2011). Lmx1a and lmx1b function cooperatively to regulate proliferation, specification, and differentiation of midbrain dopaminergic progenitors. *J. Neurosci.* **31**, 12413-12425.
Yi, S.-H., He, X.-B., Rhee, Y.-H., Park, C.-H., Takizawa, T., Nakashima, K. and Lee, S.-H. (2014). Foxa2 acts as a co-activator potentiating expression of the Nurr1-induced DA phenotype via epigenetic regulation. *Development* **141**, 761-772.
Zoli, M., Agnati, L. F., Tinner, B., Steinbusch, H. W. M. and Fuxe, K. (1993). Distribution of dopamine-immunoreactive neurons and their relationships to transmitter and hypothalamic hormone-immunoreactive neuronal systems in the rat mediobasal hypothalamus. A morphometric and microdensitometric analysis. *J. Chem. Neuroanat.* **6**, 293-310.